

Weak Gravitational lensing from regular Bardeen black holes

Hossein Ghaffarnejad¹ and Hassan niad²

Department of Physics, Semnan University, P.O.Box 35131-19111, Iran

Abstract

We consider here regular Bardeen black hole as gravitational lens and study weak deflection limits of light ray. We apply perturbation series expansion method given by Keeton et al in both regimes where the photon sphere is appeared $|q| < 0.43$ and disappeared $|q| > 0.43$. $q = g/2m$ denotes to scalar charge per ‘twice’ the mass m of the Bardeen black hole. We obtain positions and magnifications of the non-relativistic images against q . Parity of images from $|q| < 0.43$ are changed with respect to those obtained from $|q| > 0.43$. The deflection angle decreases against $|q|$. Position of the elementary images are exchanged with positions of the secondary images against increasing $|q|$. Magnification (and total magnification) of Einstein rings exhibits with discontinuity. Magnification-weighted-centroid from $|q| < 1$ is also changed with respect to those obtained from $|q| > 1$.

1 Introduction

When light ray passes from neighborhood of a massive object, it is deflected because of influence of gravity on light. This is called as gravitational lensing of light ray and encounter us to two different weak and strong limits of gravity influence on the light. These limits are distinguished by radius parameter of photon sphere corresponding to massive object (gravitational lens) such as black holes. Weak deflection limit occurs when light ray is affected by gravitational lens in far distances from photon sphere and they deflect slightly from straight line. Strong deflection limit of light ray arises by passing very close to photon sphere and turning around the lens and making relativistic images after than reaches to observer. When the light ray pass inside of (or on) photon sphere then can not escape from the gravitation of lens body and create no image. Many literatures are studied about the gravitational lensing

¹E-mail address: hghafarnejad@yahoo.com.

²E-mail address: hsniaad@gmail.com

by using analytical approach in weak deflection [1-7] and strong deflection [8-17] limits. For instance Amore et. al [18,19] and Iyer et. al [20] have studied weak and strong gravitational lensing simultaneously with analytical methods. Numerical methods is also used to study the gravitational lensing from black holes and naked singularities by Virbhadra et. al in weak and strong limits of light deflection [21-26]. Gravitational lensing is applicable basically due to the strong evidence about the presence of supermassive black holes at the center of galaxies. In the recent review article by Bozza [27] gravitational lensing are discussed with more detail, including the observational prospects.

The problem of singularities in general relativity where the theory breaks down is an important problem because the curvature scalar diverge to infinity, involving both black holes and cosmological solutions. Regular black holes are the solutions of gravity for which an event horizon is present but the space time is free from singularities. The first regular black hole was introduced by Bardeen [28] which has both event and Cauchy horizons, but with a regular center. It was shown by Borde [29-30] that the absence of the singularity is related to topology change into a de-Sitter like core. It is obtained that the Bardeen black hole is a spherically symmetric static solution of the Einstein field equations coupled to nonlinear electrodynamics source [31] and has two characteristics namely charge g and mass m . Gravitational lensing of the regular Bardeen black hole metric was studied in strong deflection limits by Eiroa and Sendra. They are used the Taylor series expansion to solve elliptical integral of the deflection angle [26] by taking into account small values of the quotient between the charge and twice the mass $|q| < 0.43$ and light rays coming from near the photon sphere. They found that when this quotient increases to limits 0.43, the relativistic images are closer to the black hole. Magnification is also decreases and the angular separation of the relativistic images grows by increasing $|q|$ to 0.43.

In this paper we have studied gravitational lensing of Bardeen black hole metric in weak deflection limit when horizons and photon sphere appears $|q| < 0.43$ and disappear $|q| > 0.43$ respectively. We use perturbation approach presented by Keeton et al [5] and obtain locations of primary and secondary non-relativistic images. Organization of the paper is as follows.

In section 2 we define the Bardeen black hole metric. We obtain Taylor series expansion of the elliptical integral of deflection angle of light ray in terms of inverse of dimensionless impact parameter $u = \frac{b}{2m} = \frac{1}{2m}|\frac{L}{E}| > 1$ where m , L and E are mass of gravitational lens, constant angular momentum and

energy of light ray respectively. We also obtain positions of the horizons (apparent and event) and photon sphere of the Bardeen black hole (the lens). In section 3 we use Virbhadra-Ellis type of lens equation and obtain its Taylor series expansion in terms of inverse of dimensionless impact parameter u . Then we determined positions of non-relativistic images. In section 4 we obtained magnification of the obtained images by using Taylor series expansion of the Magnification equation. Corresponding total and weighted-centroid magnification is also evaluated which is applicable in gravitational microlensing. In section 5 we discuss conclusion. Our obtained angles positions are re-scaled with respect to Einstein's ring angle ϑ_E throughout this paper.

2 Bardeen black holes and deflection angle

Regular black holes are that solutions of the gravity equations for which an event horizon is present, but the spacetime has not singularity. Usually they are supported by nonlinear electromagnetic fields and so have at least two characteristics namely mass m and charge g [28,32]. They are good candidates for the supermassive Galactic black holes treating as particle accelerators [33]. The first regular black hole was introduced by Bardeen such as follows.

$$ds^2 = -A(r)dt^2 + B(r)dr^2 + C(r)(d\theta^2 + \sin^2\theta d\varphi^2) \quad (2.1)$$

where

$$A(r) = 1 - \frac{2mr^2}{(r^2 + g^2)^{3/2}}, \quad B(r) = \frac{1}{A(r)}, \quad C(r) = r^2 \quad (2.2)$$

and m, g is interpreted as black hole mass and charge parameters respectively. It can be interpreted as a magnetic solution of the Einstein equations coupled to nonlinear electrodynamics [31]. Defining a dimensionless charge parameter as

$$q = \frac{g}{2m} \quad (2.3)$$

one can obtain that the Bardeen black hole reduces to Schwarzschild like for $q = 0$ and also with $q \neq 0$ for large r . Its Ricci and Kretschmann scalars are $R^\mu_\mu = 3q^2(r^2 - 4q^2)/(r^2 + q^2)^{7/2}$ and $R_{\mu\nu\eta\lambda}R^{\mu\nu\eta\lambda} = (12x^8 - 36x^6q^2 + 141x^4q^4 - 12x^2q^6 + 24q^8)/(x^2 + q^2)^7$ where $x = \frac{r}{2m}$. So it become regular in all points of the space time for $q \neq 0$ and reduces to a de sitter like space time in small r . Its horizons and photon sphere disappear for $|q| > 0.43$.

For $|q| \approx 0.39$ they are superposed (See figure 1). We will consider different values of dimensionless charge to study gravitational lensing as $|q| < 0.43$ and $|q| > 0.43$. It is convenient to use dimensionless elements of metric as

$$(2m)^{-2}ds^2 = -A(x)dT^2 + B(x)dx^2 + C(x)d\Omega^2 \quad (2.4)$$

where

$$x = \frac{r}{2m}; \quad T = \frac{t}{2m} \quad (2.5)$$

and

$$A(x) = B(x)^{-1} = 1 - \frac{x^2}{(x^2 + q^2)^{3/2}}, \quad C(x) = x^2 \quad (2.6)$$

We can obtain locations of the apparent and event horizons of the Bardeen black hole x_h by equating $A(x) = 0$ as

$$x^6 + (3q^2 - 1)x^4 + 3q^4x^2 + q^6 = 0. \quad (2.7)$$

Diagram of the above equation is plotted against q in figure 1(dot line).

The photon sphere radius x_{ps} is given by the largest positive solution of the following equation [34].

$$\frac{C'(x)}{C(x)} = \frac{A'(x)}{A(x)} \quad (2.8)$$

where over prime ' denotes to differentiation with respect to x at the point x_{ps} . Applying (2.6), the latter condition leads to the following algebraic equation.

$$4(x^2 + q^2)^5 - 9x^8 = 0. \quad (2.9)$$

Diagram of the above equation is plotted against q as solid line in figure 1.

Deflection angle of light ray coming from infinity (see figure 2) is obtained by solving the geodesic equation as

$$\hat{\alpha}(r_0) = 2\Delta\phi(r_0) - \pi \quad (2.10)$$

where $r_0 > r_{ps}$ is the closest approach distance of the light ray from center of the Bardeen black hole. Also we defined

$$\Delta\phi(r_0) = b \int_{r_0 > r_{ps}}^{\infty} \left(\frac{B(r)}{C(r)} \right)^{1/2} \left(\frac{C(r)}{A(r)} - b^2 \right)^{-1/2} dr \quad (2.11)$$

in which impact parameter b is defined as

$$b = \sqrt{\frac{C(r_0)}{A(r_0)}}. \quad (2.12)$$

Applying (2.5) and (2.6) the equations defined by (2.11) and (2.12) leads to the following form respectively

$$\Delta\phi(x_0) = \int_{x_0 \geq x_{ps}}^{\infty} \frac{x_0 dx}{x \sqrt{x^2 \left(1 - \frac{x_0^2}{(x_0^2 + q^2)^{3/2}}\right) - x_0^2 \left(1 - \frac{x^2}{(x^2 + q^2)^{3/2}}\right)}} \quad (2.13)$$

and

$$\frac{b}{2m} = \frac{x_0}{\sqrt{1 - x_0^2/(x_0^2 + q^2)^{3/2}}}. \quad (2.14)$$

Using the transformation $z = \frac{x_0}{x}$, it will be useful to rewrite (2.13) as

$$\Delta\phi = \int_0^1 \frac{dz}{\sqrt{1 - \frac{x_0^2}{(x_0^2 + q^2)^{3/2}} - z^2 + \frac{x_0^2 z^3}{(x_0^2 + q^2 z^2)^{3/2}}}} \quad (2.15)$$

which has discontinuity at $z = 1$. In limits of weak gravitational lensing where $x_0 \gg 1$ one can evaluate (2.15) by applying its Taylor series expansion about $\frac{1}{x_0}$ and integrating term by term of its coefficients such as follows.

$$\begin{aligned} \hat{\alpha}(x_0) = & \frac{2}{x_0} + \left(\frac{15\pi}{16} - 1\right) \frac{1}{x_0^2} + \left(\frac{61}{12} - \frac{15\pi}{16} - 4q^2\right) \frac{1}{x_0^3} + \\ & \left(\frac{3465\pi}{1024} - \frac{65}{8} + \left(\frac{15}{2} - \frac{315\pi}{64}\right) q^2\right) \frac{1}{x_0^4} + \\ & \left(\frac{7783}{320} - \frac{3465\pi}{512} + \left(\frac{90\pi}{8} - \frac{195}{4}\right) q^2 + 6q^4\right) \frac{1}{x_0^5} + O\left(\frac{1}{x_0^6}\right). \end{aligned} \quad (2.16)$$

The above convergent series expansion is described in terms of closest distance $x_0 > 1$ and so it is coordinate dependent. It will be useful we rewrite it in terms of coordinates invariant expression for instance impact parameter of the light ray $b = |\frac{L}{E}|$ where L and E is constants of angular momentum

and energy of light ray respectively [35]. In the latter case we can discuss observable quantities. These constants same as the black hole mass m and charge g are invariants of the light ray and so the above expansion series described by b is independent of coordinates. Furthermore we should be note that in the weak gravitational lensing approach we should be set $m/b \ll 1$ same as $x_0 \gg 1$. In the latter case we will need Taylor series expansion of the function $x_0(b)$ given by the equation (2.14) such as follows.

$$\frac{1}{x_0} = \frac{2m}{b} + \frac{1}{2} \left(\frac{2m}{b} \right)^2 + \frac{5}{8} \left(\frac{2m}{b} \right)^3 + \left(2 - \frac{3}{2} q^2 \right) \left(\frac{2m}{b} \right)^4 + \left(\frac{231}{64} - \frac{21}{4} q^2 \right) \left(\frac{2m}{b} \right)^5 + \dots \quad (2.17)$$

Substituting (2.17), the equation (2.16) leads to

$$\hat{\alpha}_q(u > 1) = \frac{A_1}{u} + \frac{A_2}{u^2} + \frac{A_3}{u^3} + \frac{A_4}{u^4} + \frac{A_5}{u^5} + \dots \quad (2.18)$$

where $u = \frac{b}{2m}$ is dimensionless impact parameter and

$$A_1 = 2, A_2 = \frac{15\pi}{16}, A_3 = \frac{4}{3}(4 - 3q^2), A_4 = \frac{315\pi}{1024}(11 - 16q^2),$$

$$A_5 = \frac{2}{5}(56 - 120q^2 + 15q^4). \quad (2.19)$$

The Taylor series expansion (2.18) remains convergent for $u > \sqrt[n]{A_n}$; $n = 1, 2, 3, \dots$ even if we choose large values $|q| > 0.43$ for which the deflection angle (2.18) is applicable for weak gravitational lensing of the Bardeen black hole with no horizons and photon sphere. Diagram of the deflection angle (2.18) is plotted against u for different values of the dimensionless scalar charge q in figure 3. This diagram shows that with fixed $|q|$, the deflection angle decreases with respect to impact parameter. We should be note that the relativistic images are made when $\alpha \geq \frac{3\pi}{2} \approx 4.71$. Thus diagrams of figure 3 are valid in the vertical axis for $\alpha < 4.71$.

We are now in position to obtain locations of non-relativistic primary and secondary images by solving the lens equation.

3 Lens equation and Image positions

We start here with Virbhadra-Ellis type of the lens equation [23,24,36] as

$$\tan \mathcal{B} = \tan \vartheta - D(\tan \vartheta + \tan(\hat{\alpha} - \vartheta)), \quad D = \frac{d_{as}}{d_s} \quad (3.1)$$

where \mathcal{B} and ϑ is the source and the image position measured from the optical axis, d_{LS} and d_S is the source-lens and source-observer distance respectively (see figure 2). One of the important quantity in study of gravitational lensing is angular radius of Einstein ring

$$\vartheta_E = \sqrt{\frac{4Gmd_{LS}}{c^2 d_L d_S}} \quad (3.2)$$

where G and c are Newton's gravitational constant and speed of light respectively. Also m and R_B are physical mass and gravitational radius of the lens respectively such that

$$R_B = \frac{2Gm}{c^2}. \quad (3.3)$$

We define now re-scaled angular parameters as

$$\beta = \frac{\mathcal{B}}{\vartheta_E}, \theta = \frac{\vartheta}{\vartheta_E}. \quad (3.4)$$

According to the postulate presented by Keeton [35] we assume that solutions of the lens equation (3.1) take Taylor series expansion as

$$\theta = \theta_0 + \theta_1 \varepsilon + \theta_2 \varepsilon^2 + \dots \quad (3.5)$$

where θ_0 is expected to be image position in the weak deflection limit and the coefficients θ_1 and θ_2 and etc. are correction terms of the image positions which should be determined. Dimensionless parameter $|\varepsilon| < 1$ is taken to be order parameter of the perturbation expansion and it was defined in terms of invariant parameters of the mass m and impact parameter b of the Bardeen black hole as

$$\varepsilon = \frac{2m}{b} = \frac{1}{u}, \quad u > 1. \quad (3.6)$$

Inserting (2.18), (2.19), (3.5) and (3.6), the equation (3.1) leads to the following coefficients.

$$\theta_0 = \frac{1}{2} \left(\beta + \sqrt{\beta^2 + 4} \right), \quad (3.7)$$

$$\theta_1 = \frac{15\pi(\beta^2 - \beta\sqrt{\beta^2 + 4} + 4)}{64(\beta^2 + 4)} \quad (3.8)$$

and

$$\theta_2 = \frac{1}{6144(\beta^2 + 4)^2} \left[(-2048D^2 - 675\pi^2 - 6144q^2 + 12288) (\beta^2 + 4)^{5/2} + \right.$$

$$3\beta (2048D^2 + 225\pi^2 + 2048q^2 - 4096) (\beta^2 + 4)^2 + 1350\sqrt{\beta^2 + 4}\pi^2 + (28672D^2 + 1350\pi^2 + 12288q^2 - 24576D - 24576) (\beta^2 + 4)^{3/2} \Big]. \quad (3.9)$$

Applying the above coefficients the relation (3.5) up to terms in order θ_3 become

$$\begin{aligned} \theta(\beta; q) \approx & \frac{1}{24576 (\beta^2 + 4)^2} \Big[(-675\pi^2 + 24064) \beta^4 - 2880\pi\beta^3 + \\ & (-4050\pi^2 + 162816) \beta^2 - 11520\pi\beta - 4050\pi^2 + 266240 \Big] \sqrt{\beta^2 + 4} + \\ & (675\pi^2 + 1536) \beta^5 + 2880\pi\beta^4 + (5400\pi^2 + 12288) \beta^3 + 23040\pi\beta^2 + \\ & (10800\pi^2 + 24576) \beta + 46080\pi \Big] - \frac{\left((\beta^2 + 2) \sqrt{\beta^2 + 4} - \beta (\beta^2 + 4) \right) q^2}{4\beta^2 + 16} \end{aligned} \quad (3.10)$$

where we set $D = 0.5$ and $\varepsilon = 0.5$. Diagram of the above image position equation is plotted against β in figure 4 for given different values of the dimensionless charge q . In cases $\beta \leq 0$ the diagrams show exchange of positions of the elementary and secondary images (the parity) where we choose particular values $|q| < 1$ and $|q| > 1$ respectively. Positions of the Einstein rings $\theta_q(0) = \theta_E$ are determined on the vertical axes of the figure 4 with $\beta = 0$. Corresponding equation is given in terms of the parameters D , q and ε such as follows.

$$\theta_E = 1 + \frac{15\pi\varepsilon}{64} + \left(\frac{20D^2}{12} - 2D - \frac{675\pi^2}{8192} - q^2 + 2 \right) \varepsilon^2 + \dots \quad (3.11)$$

It should be noted that with fixed β primary images θ^+ correspond to choices $\beta > 0$ and secondary images θ^- correspond to $\beta < 0$ and they are formed in opposite side of the lens such that $\theta^-(\beta) = \theta^+(-\beta)$. When we choose $|q| < 0.43$ ($|q| > 0.43$) the images are formed in the presence (absence) of photon sphere and horizon of the Bardeen black hole. In the next section we study magnifications of the determined images.

4 Magnifications

It is well known that the gravitational lensing conserves surface brightness (because of Liouville's theorem), but gravitational lensing changes the ap-

parent solid angle of a source. The total flux received from a gravitationally lensed image of a source is therefore changed in proportion to the ratio between the solid angles of the image and the source which is called magnification of images with respect to corresponding source. It is evaluated by

$$\mu = \left| \frac{\sin\beta}{\sin\theta} \frac{d\beta}{d\theta} \right|^{-1} \quad (4.1)$$

in which the tangential and radial magnification are given by $\mu_t = (\frac{\sin\beta}{\sin\theta})^{-1}$ and $\mu_r = (\frac{d\beta}{d\theta})^{-1}$ respectively. We need now to expand μ with respect to the order parameter ε such as follows.

$$\mu = \mu_0 + \mu_1\varepsilon + \mu_2\varepsilon^2 + \dots \quad (4.2)$$

where

$$\mu_0 = \frac{(\beta^2 + 2) \sqrt{\beta^2 + 4} + \beta (\beta^2 + 4)}{2\beta (\beta^2 + 4)}, \quad (4.3)$$

$$\mu_1 = -\frac{15\pi}{32 (\beta^2 + 4)^{3/2}} \quad (4.4)$$

and

$$\begin{aligned} \mu_2 = \frac{1}{3072\beta (\beta^2 + 4)^3} & \left[-\sqrt{\beta^2 + 4} (2048D^2\beta^4 + 61440D^2\beta^2 + 2025\pi^2\beta^2 + \right. \\ & 18432\beta^2q^2 - 36864(D)\beta^2 + 180224D^2 + 8100\pi^2 - 36864\beta^2 + 61440q^2 - 122880D \\ & \left. - 122880) + \beta (\beta^2 + 4) (16384D^2 + 2025\pi^2 + 6144q^2 - 12288D - 12288) \right]. \end{aligned} \quad (4.5)$$

The above coefficients have positive parity μ^+ because they are related to primary images θ^+ . In order to derive magnification with negative parity μ^- obtained from secondary images θ^- , we must replace β in the equation (4.2) with $-\beta$ as

$$\mu^-(\beta) \equiv \mu^+(-\beta). \quad (4.6)$$

In cases similar to microlensing made from distant sources for which the positions of primary and secondary images are so close and practically inextricable, total magnification μ_{tot} and magnification-weighted centroid μ_{cent} are two main factor to study gravitational lensing such that

$$\mu_{tot} = |\mu^+| + |\mu^-| \quad (4.7)$$

and

$$\mu_{cent} = \frac{\theta^+ |\mu^+| + \theta^- |\mu^-|}{|\mu^+| - |\mu^-|}. \quad (4.8)$$

Applying (4.2), (4.3), (4.4), (4.5) and (4.6) one can obtain Taylor series expansion of the equations (4.7) and (4.8) respectively such as follows.

$$\begin{aligned} \mu_{tot} = & \frac{\beta^2 + 2}{\beta \sqrt{\beta^2 + 4}} + \frac{1}{4} \left[1024 (\beta^2 + 4) (\beta^2 + 18) D^2 + 6144 (\beta^2 + 4) (q^2 - 2D) \right. \\ & \left. + 2025\pi^2 - 12288\beta^2 - 49152 \right] \varepsilon^2 + \dots \end{aligned} \quad (4.9)$$

and

$$\begin{aligned} \mu_{cent} = & \frac{(\beta^2 + 3) \beta}{\beta^2 + 2} - \frac{\beta (\beta^2 + 2)^5}{1536 (\beta^2 + 4)^8} \left[-1024 (\beta^2 + 4) (\beta^4 + 9\beta^2 - 2) D^2 \right. \\ & \left. + 2025\pi^2 + 6144\beta^2 (\beta^2 + 4) D + 6144 (q^2 - 2) (\beta^2 + 4) \right] \varepsilon^2 + \dots \end{aligned} \quad (4.10)$$

Setting $D = 0.5, \varepsilon = 0.5$ and applying (4.3), (4.4) and (4.5), one can rewrite the magnification (4.2) exactly in terms β and q as

$$\begin{aligned} \mu[\theta_0(\beta); q] \approx & \frac{\theta_0^4}{\theta_0^4 - 1} - \frac{15\pi\theta_0^3}{64 (\theta_0^2 + 1)^3} + \frac{1}{6144 (\theta_0^2 (\theta_0^2 + 1)^2 - 1)^5} \times \\ & \left[\theta_0^2 (6144q^2\theta_0^6 + 256\theta_0^8 + 2025\pi^2\theta_0^4 + 12288q^2\theta_0^4 - 13824\theta_0^6 + \right. \\ & \left. 6144\theta_0^2q^2 - 28160\theta_0^4 - 13824\theta_0^2 + 256) \right] + \dots \end{aligned} \quad (4.11)$$

where $\theta_0(\beta)$ should be inserted from the equation (3.7). Setting $D = 0.5, \varepsilon = 0.5$ one can obtain total magnification (4.9) and magnification-weighted centroid (4.10) respectively as

$$\begin{aligned} \mu_{tot}(\beta; q) \approx & \frac{\beta^2 + 2}{\beta \sqrt{\beta^2 + 4}} + \frac{1}{16} \left[256 (\beta^2 + 4) (\beta^2 + 18) + 6144 (\beta^2 + 4) (q^2 - 1) \right. \\ & \left. + 2025\pi^2 - 12288\beta^2 - 49152 \right] + \dots \end{aligned} \quad (4.12)$$

and

$$\mu_{cent}(\beta; q) \approx \frac{(\beta^2 + 3)\beta}{\beta^2 + 2} - \frac{\beta(\beta^2 + 2)^5}{6144(\beta^2 + 4)^8} \left[-256(\beta^2 + 4)(\beta^4 + 9\beta^2 - 2) \right. \\ \left. + 2025\pi^2 + 3072\beta^2(\beta^2 + 4) + 6144(q^2 - 2)(\beta^2 + 4) \right] + \dots \quad (4.13)$$

We have plotted diagrams of the equations (4.11), (4.12) and (4.13) in figures 5, 6 and 7 respectively by regarding different values of the dimensionless charge q . Diagrams of the figures 5, 6 and 7 show that parity of the images obtained with $|q| < 1$ are exchanged with those obtained from $|q| > 1$. Also the magnification of images of the Einstein rings reduces to infinity for different values of the charge parameter $|q|$. Absolute value of magnifications is eliminated for the Einstein rings but grows for larger values $|q|$ against increasing $|\beta|$. However magnification-weighted-centroid has same variation in terms of the source position by increasing $|q|$.

5 Concluding remarks

In this paper, we have obtained the weak limit of light ray deflection angles against impact parameter for regular Bardeen black hole lens. This lens contains two characteristics namely charge g and mass m and our study follows all values $|q| = \frac{|g|}{2m} > 0$. Black hole horizons and corresponding photon sphere appear (disappear) with $|q| < 0.43$ ($|q| > 0.43$). We used perturbation series expansion method presented by Keeton et al and obtained Taylor series expansion of the non-relativistic elementary and secondary image positions, corresponding magnifications (total and centroid) as functions of the source position β . Physical effects of the charge per mass quantity $|q|$ is obtained on the image parity and angle positions of the Einstein's rings. We have found that when $|q|$ increases, the deflection angle decreases. Increasing $|q|$ with a fixed source position, the non-relativistic image positions are closer and primary image locations transmit to corresponding secondary image positions. Absolute value of magnification of the images grows with respect to positions of the source against increasing $|q|$. However magnification-weighted-centroid remains as invariant property of our gravitational lensing system under the increase of dimensionless charge $|q|$ and source positions. Same results were obtained previously by Eiroa et al [17] by studying strong

deflection limit of the problem. They obtained that when $|q|$ increases the relativistic images are closer to the Bardeen black hole.

References

1. P. Schneider, J. Ehlers and E. E. Falco, *Gravitational lenses*, Springer-Verlag, Berlin (1992).
2. A. O. Petters, H. Levine and J. Wambsganss, *Singularity Theory and Gravitational Lensing*, Boston-Birkhauser, (2001).
3. R. Epstein and I. I. Shapiro, Phys. Rev. D 22, 2947 (1980).
4. M. Sereno, Phys. Rev. D 69, 023002 (2004).
5. C. R. Keeton and A. O. Petters, Phys. Rev. D 72, 104006 (2005).
6. M. Sereno and F. De Luca, Phys. Rev. D 74, 123009 (2006).
7. M. C. Werner and A. O. Petters, Phys. Rev. D 76, 064024 (2007).
8. S. Frittelli, T. P. Kling, and T. Newman, Phys. Rev. D 61, 064021 (2000).
9. V. Bozza, Phys. Rev. D 66, 103001 (2002).
10. V. Bozza, Phys. Rev. D 67, 103006 (2003).
11. V. Bozza, F. De Luca, G. Scarpetta, and M. Sereno, Phys. Rev. D 72, 083003 (2005).
12. V. Bozza, F. De Luca, and G. Scarpetta, Phys. Rev. D 74, 063001 (2006).
13. R. Whisker, Phys. Rev. D 71, 064004 (2005).
14. E. F. Eiroa, Phys. Rev. D 71, 083010 (2005).
15. E. F. Eiroa, Phys. Rev. D 73, 043002 (2006).
16. K. Sarkar and A. Bhadra, gr-qc/0602087.
17. Eiroa, E.F. and Sendra. C.M., Class. Quantum Grav. 28, 085008 (2011).
18. Amore, P., and Arceo, S. Phys. Rev. D, 73, 083004, (2006).

19. Amore, P., Arceo, S., and Fernandez, F. M. Phys. Rev. D, 74, 083004, (2006).
20. Iyer, S. V., and Petters, A.O., Gen. Relativ. Gravit., 39, 1563, (2007).
21. Virbhadra, K. S., and Keeton, C. R., Phys. Rev. D, 77, 124014, (2008).
22. Virbhadra, K.S., Int. J. Mod. Phys. A, 12, 4831, (1997).
23. Virbhadra, K.S., Phys. Rev. D, 79, 083004, (2009).
24. Virbhadra, K.S., and Ellis, G.F.R., Phys. Rev. D, 62, 084003, (2000).
25. Virbhadra, K.S., and Ellis, G.F.R., Phys. Rev. D, 65, 103004, (2002).
26. Virbhadra, K.S., Narasimha, D., and Chitre, S.M., Astron. Astrophys., 337, (1998).
27. Bozza V. Gen, Rel. Grav. 42, 2269 (2010).
28. Bardeen J, Proc. GR5 (Tiflis, USSR) (1968).
29. Borde A. Phys. Rev. D50, 3692 (1994).
30. Borde A. Phys. Rev. D55, 7615 (1997).
31. Ayon Beato E and Garcia A, Phys. Lett. B493, 149 (2000).
32. Ansoldi S, gr-qc/0802.0330 (2008).
33. Pradhan P., gr-qc/1402.2748v2 (2014).
34. Weinberg S, *Gravitation and Cosmology: Principles and Applications of the General Theory of Relativity (New York, Wiley (1972))*.
35. C. R. Keeton and A. O. Petters, Phys. Rev. D 72, 104006 (2005).
36. V. Bozza, Phys. Rev. D78, 103005 (2008).

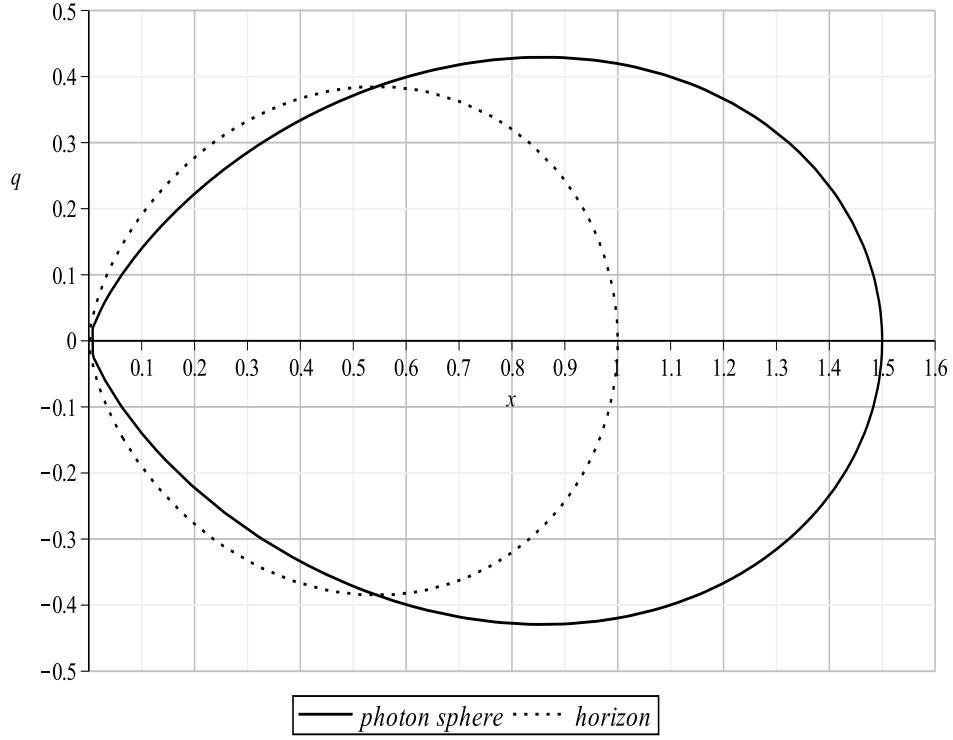


Figure 1: Diagram of locations of the horizons (event and apparent) are plotted with dot-line and location of corresponding photon sphere radius is plotted with solid-line respectively for different values of the charge q . Fixing q with particular value one can determine position of the photon sphere with largest positive value on the horizontal axis. $|q| \approx 0.39$ corresponds to $x_{ps} = x_h \approx 0.55$.

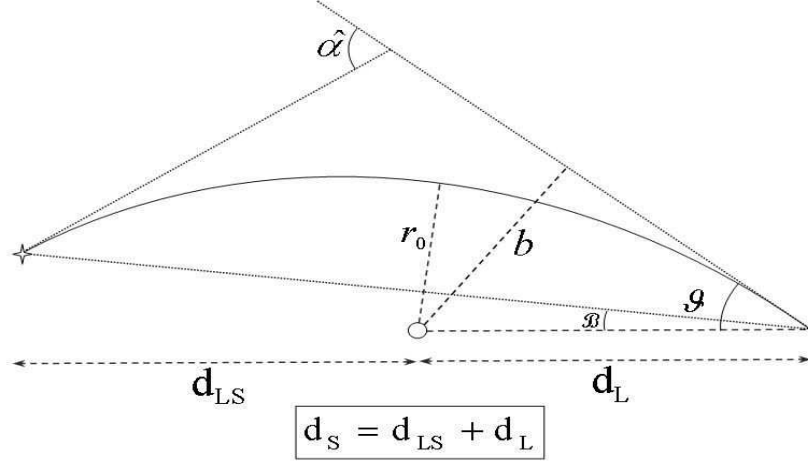


Figure 2: Diagram shows gravitational lensing perspective via spherically symmetric static body. β and θ is angular position of the source and the image measured from the optical axis. d_{LS} and d_S is the source-lens and source-observer distance respectively. $b = |L/M|$ is impact parameter in which the constants L and E is angular momentum and energy of the light ray. r_0 is closest approach distance of the light ray and α is deflection angle.

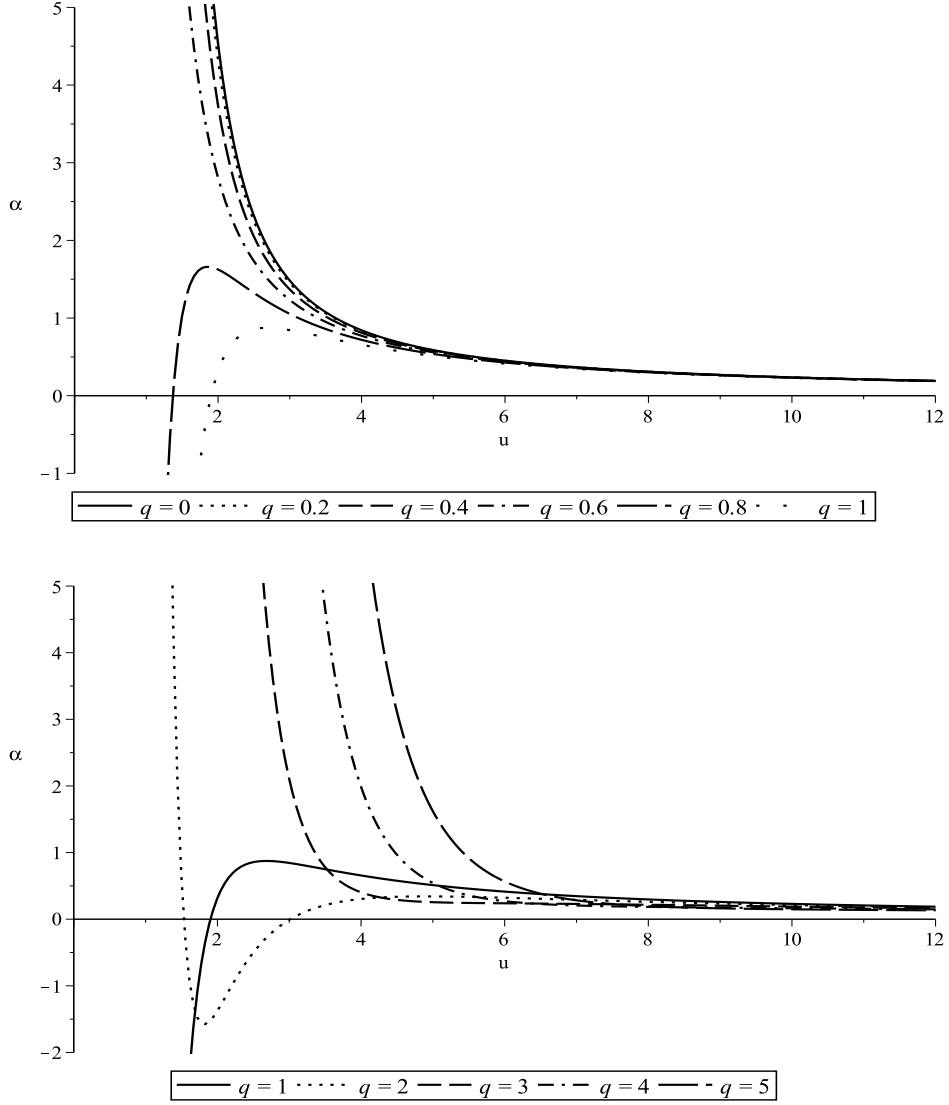


Figure 3: Variation of the deflection angle α is plotted against dimensionless impact parameter $u = \frac{b}{2m}$ for $0 < q < 5$.

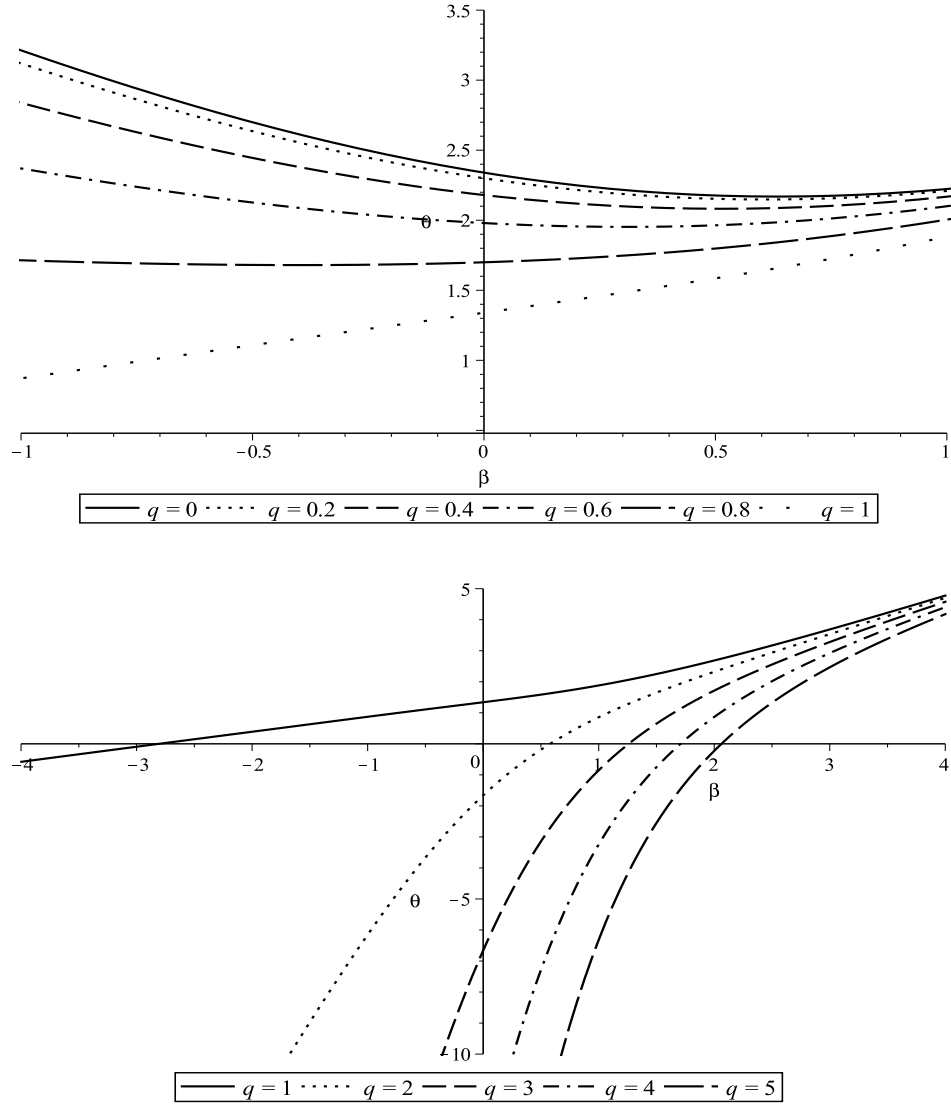


Figure 4: Image positions θ are plotted against source positions β for $0 < q < 5$.

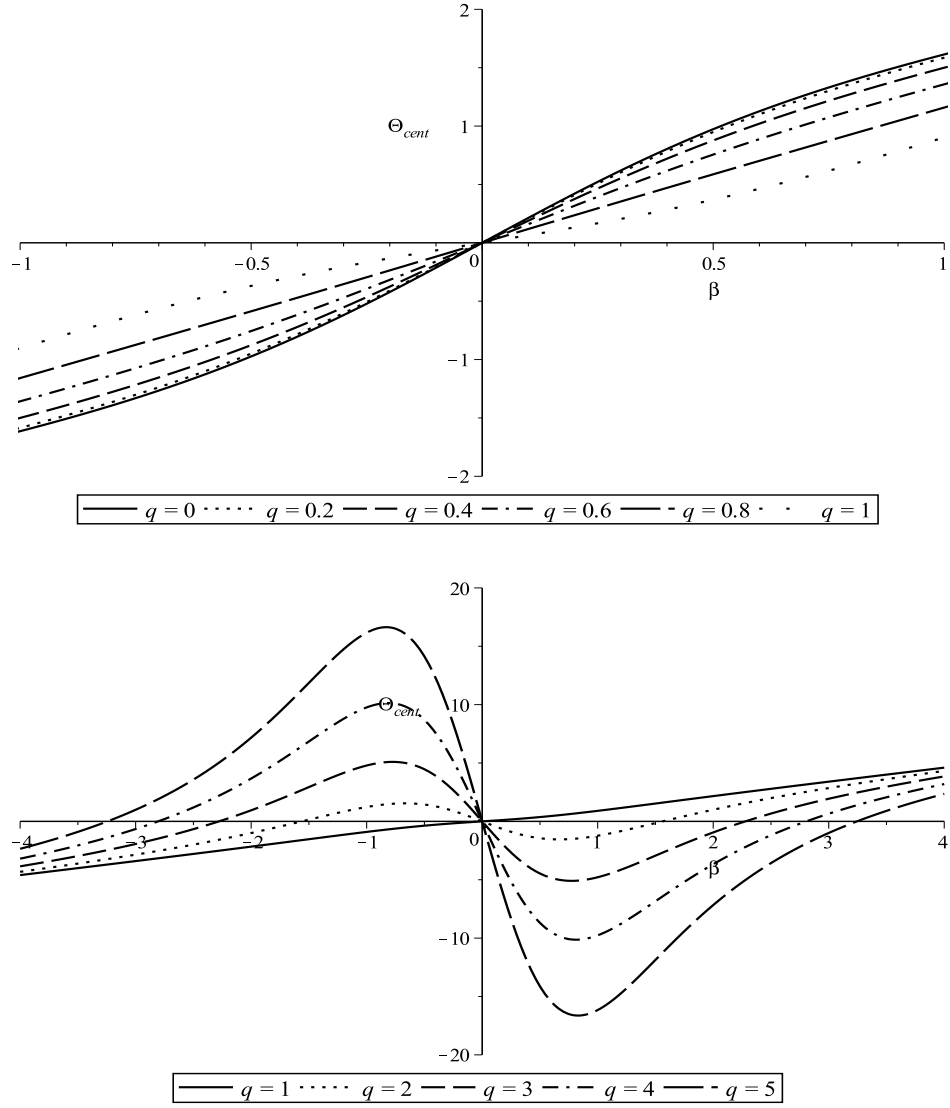


Figure 5: Magnification μ is plotted against source positions β for $0 < q < 5$.

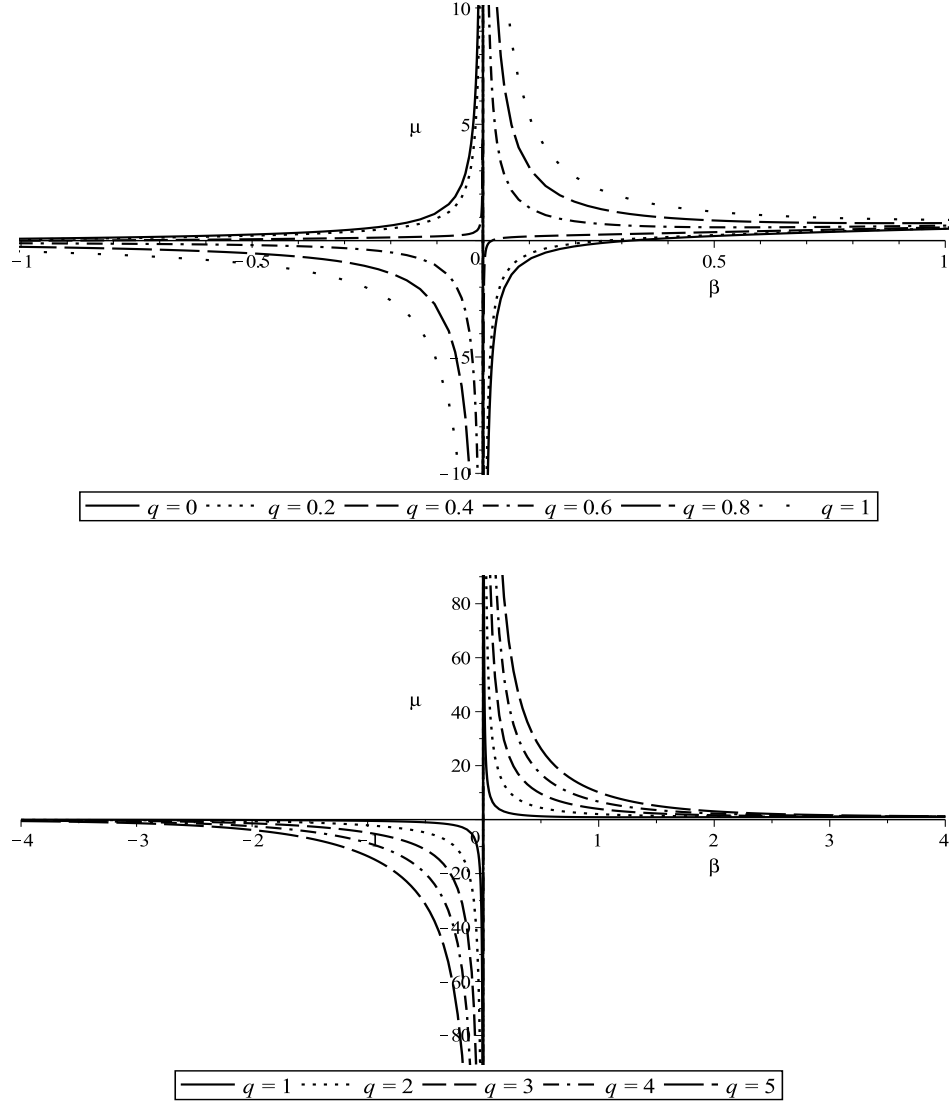


Figure 6: Total magnification μ_{tot} is plotted against position of the source β for $0 < q < 5$.

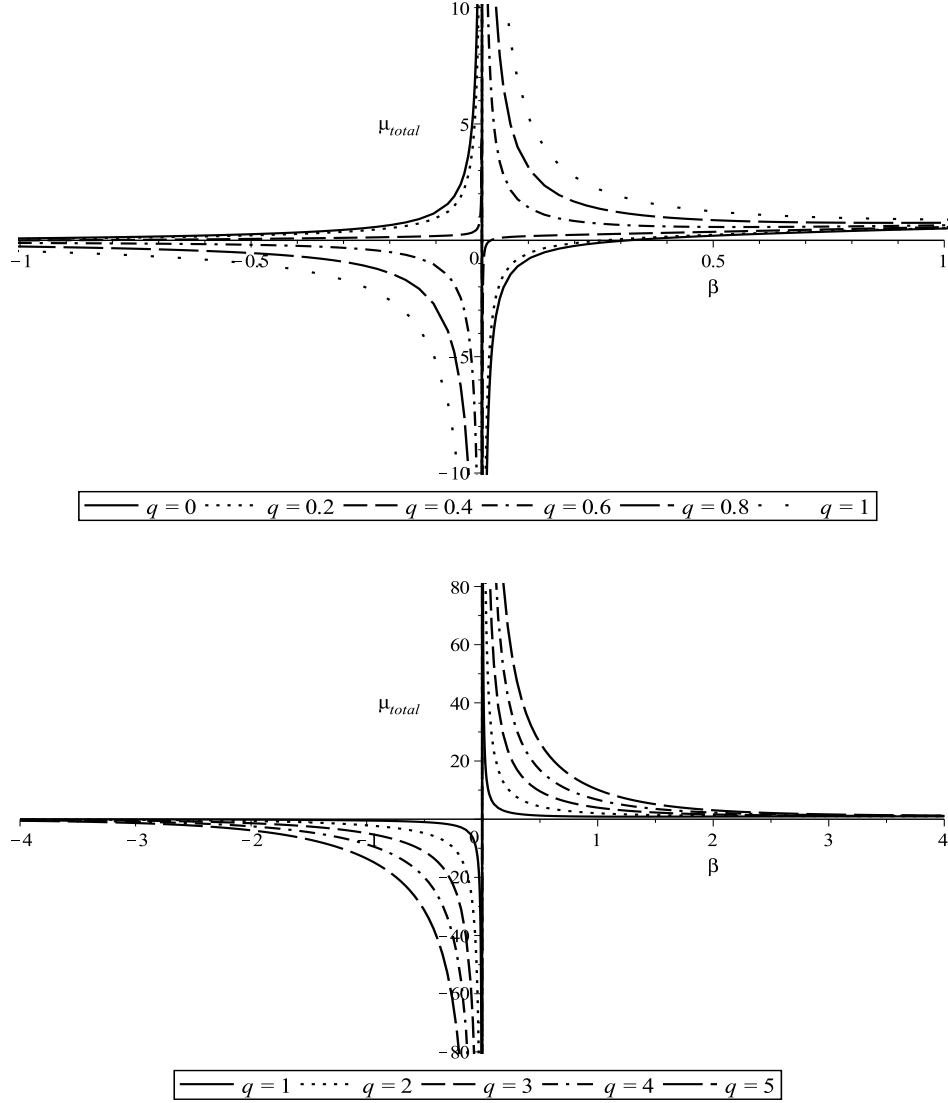


Figure 7: The magnification-weighted centroid μ_{cent} is plotted against position of the source β for $0 < q < 5$.